

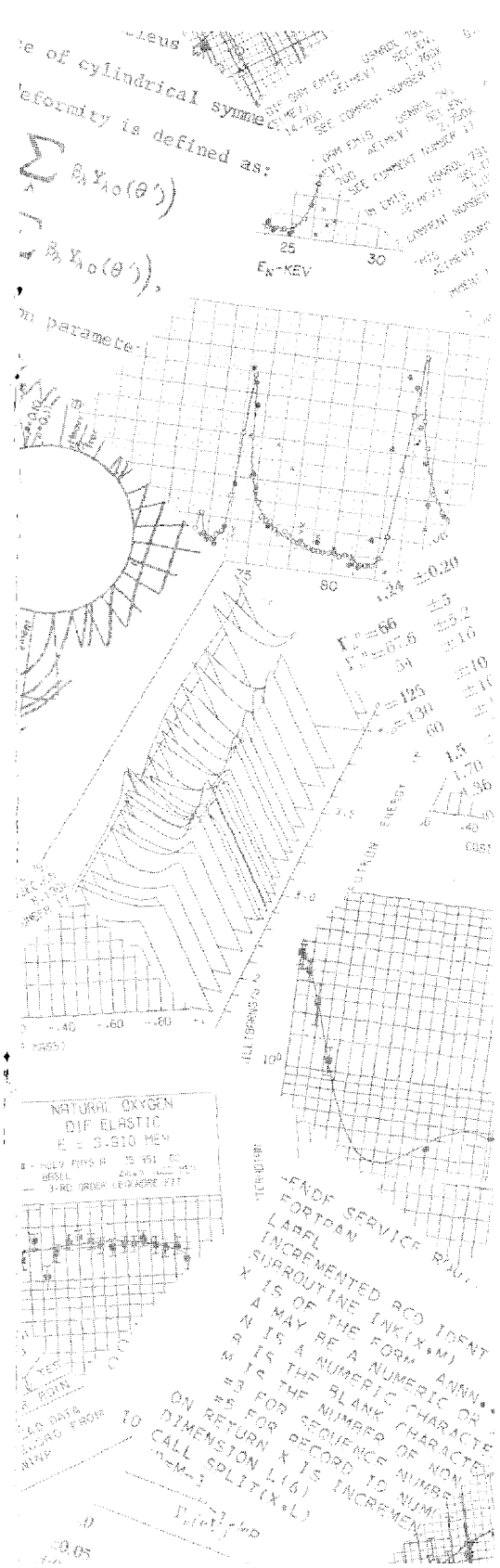
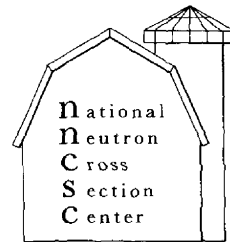
BNL 50439
(ENDF-215)

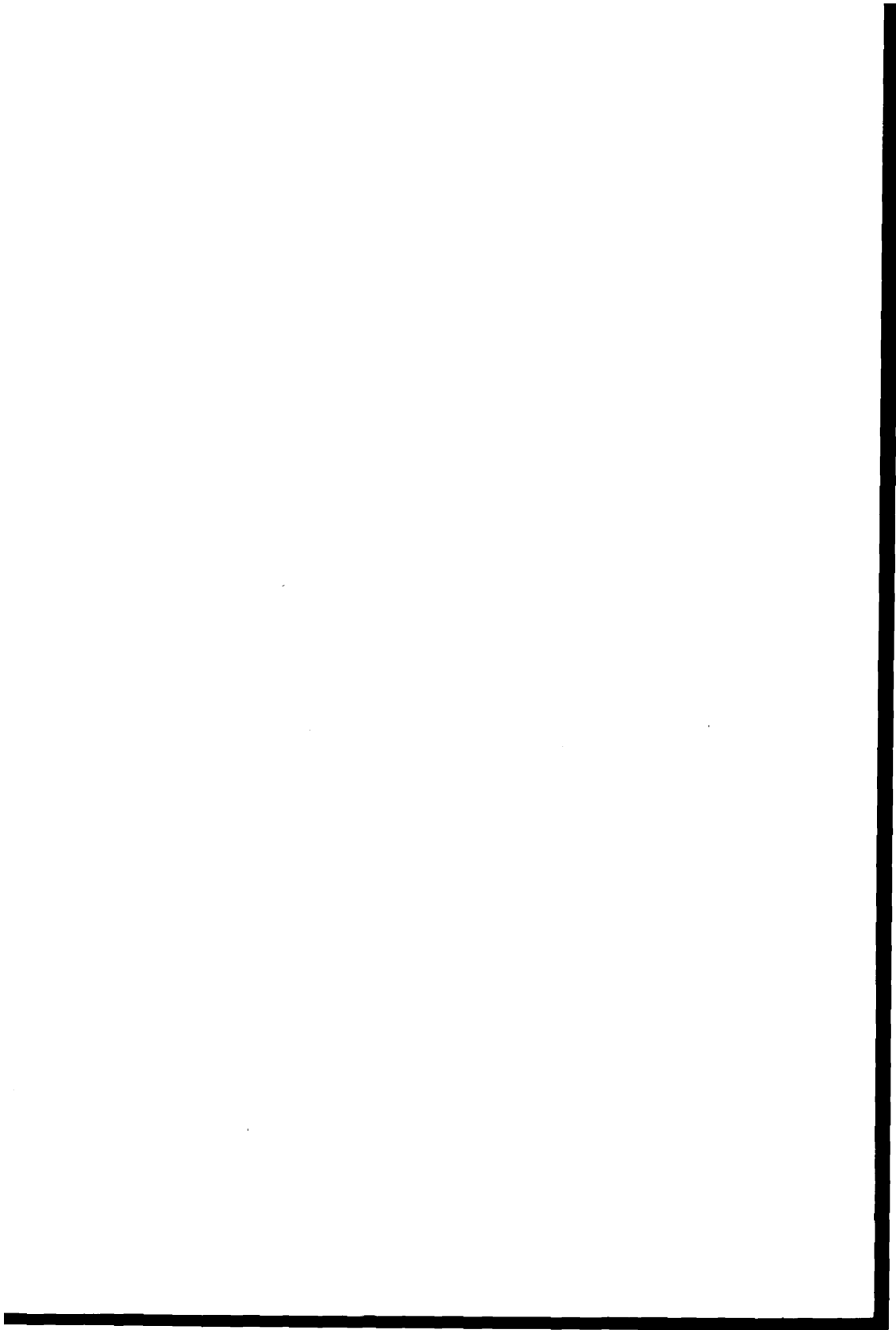
EVALUATED NEUTRON CROSS SECTIONS OF ^{197}Au

S.F. MUGHABGHAB, A. PRINCE, M.D. GOLDBERG,
M.R. BHAT AND S. PEARLSTEIN

October 1974

NATIONAL NEUTRON CROSS SECTION CENTER
BROOKHAVEN NATIONAL LABORATORY
UPTON, NEW YORK 11973





BNL 50439
(ENDF-215)
(Physics-Nuclear - TID-4500)

EVALUATED NEUTRON CROSS SECTIONS OF ^{197}Au

S.F. MUGHABGHAB, A. PRINCE, M.D. GOLDBERG, M.R. BHAT AND S. PEARLSTEIN



October 1974

NATIONAL NEUTRON CROSS SECTION CENTER
BROOKHAVEN NATIONAL LABORATORY
ASSOCIATED UNIVERSITIES, INC.

UNDER CONTRACT NO. AT(30-1)-16 WITH THE
UNITED STATES ENERGY RESEARCH AND DEVELOPMENT ADMINISTRATION

NOTICE

This report was prepared as an account of work sponsored by the United States Government. Neither the United States nor the United States Energy Research and Development Administration, nor any of their employees, nor any of their contractors, subcontractors, or their employees, makes any warranty, express or implied, or assumes any legal liability or responsibility for the accuracy, completeness or usefulness of any information, apparatus, product or process disclosed, or represents that its use would not infringe privately owned rights.

Printed in the United States of America
Available from
National Technical Information Service
U.S. Department of Commerce
5285 Port Royal Road
Springfield, VA 22161
Price: Printed Copy \$4.00; Microfiche \$1.45
January 1975 525 copies

Contents

	Page
I. Introduction	1
II. Resolved Resonance Parameters	2
III. Smooth Neutron Cross Sections	3
(1) Total Cross Section	3
(2) Elastic Cross Section	5
(3) Capture Cross Section	5
(4) Inelastic Scattering Cross Section	16
(5) (n, particle) Cross Section	18
(a) (n,2n) Cross Section	19
(b) (n,3n) Cross Section	19
(c) (n,p) Cross Section	23
(d) (n, α) Cross Section	23
IV. Angular Distribution of Secondary Neutrons	26
V. Energy Distribution of Secondary Neutrons	31
VI. Summary and Conclusions	32
Acknowledgement	34
References	35

List of Tables

No.	Title	Page
1	Resonance Parameters of ^{197}Au	4

List of Illustrations

No.	Title	Page
1	Capture Cross Section of ^{197}Au in energy range from thermal to 100 eV.	3
2	Total Cross Section 10-100 keV	6
3	Total Cross Section 0.10-1.0 MeV	7
4	Total Cross Section 1.0-5.0 MeV	8
5	Total Cross Section 5.0-20.0 MeV	9
6	Non-Elastic Cross Section 0-20 MeV	10
7	Capture Cross Section 1-20 keV	10
8	^{235}U fission Cross Section 25-100 keV	11
9	Averaged ^{235}U fission Cross Section 25-100 keV	11
10	Capture Cross Section 10-100 keV	12
11	Capture Cross Section 100 keV-1 MeV	13
12	Capture Cross Section 0.5-3.0 MeV	14
13	Energy Levels of ^{197}Au	18
14	Inelastic Cross Section, exciting the 77.4 keV level	20
15	Inelastic Cross Section exciting the combined levels at 269 and 279 keV	20
16	Inelastic Cross Section exciting the 409 keV level	20
17	Inelastic Cross Section exciting the combined levels at 503 and 518 keV	20
18	Inelastic Cross Section exciting the level at 737 keV	21
19	Inelastic cross Section exciting the combined levels at 856 and 889 keV	21
20	Inelastic Cross Section exciting the 1045 keV level	21
21	Inelastic Cross Section exciting the combined levels at 1121 and 1151 keV	21
22	Inelastic Cross Section exciting the combined levels at 1218 and 1242 keV	22
23	The (n,2n) and (n,3n) Cross Sections	22
24	The (n,p) Cross Section	24
25	The (n, α) Cross Section	25
26	Elastic Angular Distribution for $E_n=0.5$ MeV	27
27	Elastic Angular Distribution for $E_n=1.0$ MeV	28
28	Elastic Angular Distribution for $E_n=2.5$ MeV	29
29	Elastic Angular Distribution for $E_n=5.0$ MeV	30

I. Introduction

Because of the importance of gold as a standard in cross section measurements, and in order to update the evaluated nuclear data files, a new evaluation of the neutron cross sections of gold was undertaken. This evaluation for ENDF/B-IV differs from the previous (ENDF/B-III) evaluation in the following respects:

- (a) the high energy limit of resonance region has been extended from 995.4 eV to 2 keV.
- (b) the parameters of a bound level have been derived so that it is not necessary to add in a $1/v$ cross section in the low energy range.
- (c) the calculated resonance capture integral, I_γ , from the present resonance parameters and from the capture cross section in the higher energy region is in better agreement with the recommended experimental value, 1560 ± 40 b. Calculations of I_γ , with the aid of RESEND using ENDF/B-III yielded $I_\gamma = 1600$ b.
- (d) In ENDF/B-III, inelastic excitation of the 77.8 keV level only was supplied. In the present evaluation, inelastic scattering data are extended up to an excitation energy of 1242 keV.
- (e) The present capture cross section data seem to be in better shape than previously. For example, in the energy range 20-600 keV the uncertainty in the capture cross section of Au is possibly as low as 4%.
- (f) For the (n, particle) reactions, very few additional measurements are available. The new measurements are mainly for the (n,2n) reactions at an energy of about 14 MeV.

II. Resolved Resonance Parameters

The recommended resonance parameters in the energy range 4.9 eV - 2 keV, which appeared in BNL-325, 3rd edition,⁽¹⁾ were adopted with minor changes and additions. The recent spin assignments of Lottin and Jain⁽²⁾ were incorporated, and the parameters of a bound level were derived in order to fit the experimental capture and total cross sections at low neutron energies. The capture cross section at $E_n = 0.0253$ eV was constrained to a value of 98.8 b. Furthermore, a spin assignment of $J = 2$ for the bound level was assumed. This spin was deduced by Wasson et al⁽³⁾ from interference analysis of neutron capture γ rays. Fig. 1 illustrates the calculated capture cross section in the energy range 0.0001-100 eV compared with the experimental data. The calculated curve is based on the Breit-Wigner single level formalism. Doppler and resolution broadening were not applied. Note that throughout the energy range depicted in Fig. 1, and particularly for $E_n < 10$ eV, good agreement is achieved with the data of Haddad et al⁽⁴⁾.

Table 1 gives a summary of the resonance parameters. In those cases where spin assignments are not determined experimentally, spin values were selected randomly in such a manner that the $2J+1$ law of level density is obeyed. The resonance parameters of Macklin et al⁽⁵⁾ and Hacken et al⁽⁶⁾ were not yet available at the time the evaluation was completed.

The capture resonance integral calculated with the aid of INTER code using the resolved resonance parameters of Table 1 is 1559 b. The low energy cut-off was taken as 0.5 eV. The contribution from the higher energy region, from 2 keV to 20 MeV, is 6 b. This results in a total capture integral of 1565 b which is in excellent agreement with the recommended value⁽¹⁾ of 1560 ± 40 b. The unresolved region extends from 2-10 keV. Spin independent S-wave and p-wave strength functions, S_0 and S_1 , respectively are used. These are as follows:

$$S_0 = 2.1 \times 10^{-4}$$

$$S_1 = 0.4 \times 10^{-4}$$

In addition, in this energy region, average level spacings for s and p wave levels are described by:

$$D = \frac{D_0}{2J+1}$$

where $D_0 = 129.6$ eV.

A constant average radiative width, $\Gamma_\gamma = 0.125$ eV, for s- and p- wave resonances is assumed in the calculations.

III. Smooth Neutron Cross Sections

(1) Total Cross Section

As pointed out previously, the resolved resonance region extends up to about 2 keV and the unresolved region from 2 to 10 keV. From 10 keV to 20 MeV, the evaluated total cross section curve was obtained by making a spline fit to the various sets of available experimental data. Thus, from 10 keV to

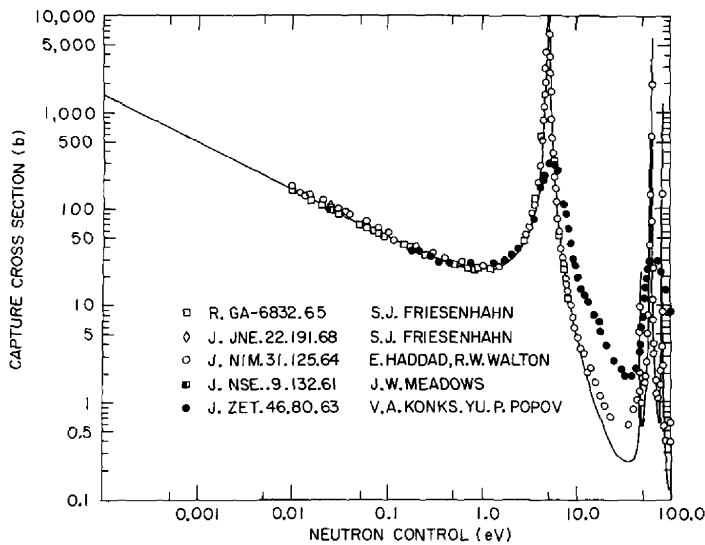


Figure 1. Capture Cross Section of ^{197}Au in energy range from thermal to 100 eV.

Table 1

E_o (eV)	J	Γ (mV)	Γ_n (mV)	Γ_Y (mV)	E_o (eV)	J	Γ (mV)	Γ_n (mV)	Γ_Y (mV)	E_o (eV)	J	Γ (mV)	Γ_n (mV)	Γ_Y (mV)
25.58	2	176.42	52.4195	124	628.40	2	160.00	22.00	138	1310.70	2	377.00	253.00	124
4.906	2	139.20	15.20	124	638.70	2	630.00	480.00	150	1328.80	1	840.00	704.00	136
46.45	1	124.13	0.13	124	658.70	1	130.40	6.40	124	1335.80	2	249.00	125.00	124
58.10	1	116.40	4.40	112	685.90	1	137.30	13.30	124	1354.30	1	720.00	592.00	128
60.30	2	198.00	68.00	130	695.80	1	830.00	667.00	163	1359.50	2	150.00	26.00	124
78.40	1	146.70	16.70	130	699.00	2	880.00	736.00	144	1367.70	1	391.00	267.00	124
107.00	2	127.80	7.80	120	715.60	2	285.0	115.0	170	1395.80	2	156.00	32.00	124
122.3	2	124.80	0.80	124	738.40	2	132.00	8.00	124	1426.20	1	285.00	261.00	124
144.20	1	128.90	8.90	120	759.90	1	581.00	427.00	154	1428.80	2	550.00	426.00	124
151.30	2	142.00	22.00	120	773.80	1	600.00	475.00	125	1450.50	2	410.00	277.00	133
162.90	1	180.00	50.00	130	784.30	2	280.00	120.00	160	1469.20	2	161.00	37.00	124
164.90	2	115.30	9.30	106	796.00	2	325.00	178.00	147	1474.30	1	284.00	160.00	124
190.30	2	174.00	44.0	130	813.50	1	146.00	22.00	124	1490.40	2	1160.00	1035.00	125
209.30	2	124.58	0.58	124	819.50	2	380.00	230.00	150	1501.50	1	154.40	30.40	124
240.50	2	172.00	72.00	100	825.00	2	700.00	533.00	167	1530.00	1	174.00	50.00	124
255.70	1	124.80	0.80	124	864.50	1	170.0	23.00	147	1552.30	2	300.00	150.00	150
262.40	1	253.00	133.00	120	879.70	2	170.0	35.00	135	1569.60	1	136.00	12.00	124
273.60	2	109.20	4.20	105	932.40	2	560.00	411.00	149	1578.40	1	640.00	480.00	160
293.00	2	511.00	365.00	146	961.30	1	260.00	109.00	151	1593.30	2	183.00	59.00	124
329.50	2	279.60	45.60	134	984.20	2	480.00	331.00	149	1614.40	2	280.00	166.00	114
331.00	1	200.00	62.00	138	988.60	2	290.00	121.00	169	1641.50	1	244.00	120.00	124
355.00	2	164.20	39.20	125	995.50	2	650.00	496.00	154	1646.40	2	220.00	96.00	124
370.70	2	190.00	84.00	106	1022.40	1	125.30	1.30	124	1660.50	1	130.10	6.10	124
375.10	1	143.90	13.90	130	1039.60	1	168.00	44.00	124	1693.20	2	258.00	134.00	124
381.50	2	166.10	61.10	105	1043.00	1	610.00	485.00	125	1706.20	2	394.00	270.00	124
400.00	2	160.00	20.00	140	1063.90	2	130.40	6.40	124	1721.20	2	161.00	37.00	124
440.00	1	420.00	288.00	132	1077.70	1	484.00	360.00	124	1734.40	2	439.00	315.00	124
450.90	2	172.00	62.00	110	1092.50	2	520.00	376.00	144	1754.50	2	444.00	320.00	124
477.00	2	450.00	320.00	130	1120.40	1	146.00	22.00	124	1756.30	1	692.00	568.00	124
490.00	1	187.00	57.00	130	1128.60	2	161.00	37.00	124	1811.40	1	220.00	96.00	124
494.00	2	160.00	27.00	133	1135.4	2	490.00	339.00	151	1821.10	2	138.00	140.00	124
534.10	2	162.00	35.00	127	1177.50	2	132.00	8.00	124	1832.00	1	212.00	88.00	124
548.60	1	180.00	53.00	127	1183.00	2	430.00	290.00	140	1856.30	1	1550.00	1383.00	167
579.10	2	520.00	37.00	150	1207.00	2	500.00	360.00	140	1860.00	2	210.00	86.00	124
580.90	1	262.00	147.00	115	1218.50	2	156.00	32.00	124	1883.60	1	351.00	227.00	124
587.00	2	169.00	35.00	134	1223.30	1	700.00	560.00	140	1893.30	2	127.70	3.70	124
602.80	2	369.00	224.00	145	1245.40	1	257.00	133.00	124	1913.60	1	2600.00	2453.00	147
617.30	2	234.00	74.00	160	1281.70	1	600.00	459.00	141	1939.70	1	650.00	520.00	130
624.80	1	170.00	49.00	121	1288.00	2	139.00	15.00	124	1960.90	2	900.00	734.00	166

1.0 MeV (Figs. 2 and 3) the low energy data of Seth⁽⁷⁾, Bilpuch⁽⁸⁾, Whalen⁽⁹⁾, Day⁽¹⁰⁾, and Walt and Becker⁽¹¹⁾ were used. The measurements of Snowdon⁽¹²⁾ were not included since they were considered too high. From 1.0 MeV to 16.0 MeV, the smooth cross section curve was determined by the data of Foster⁽¹³⁾, Walt and Becker⁽¹¹⁾, Walt⁽¹⁴⁾, Nereson⁽¹⁵⁾, Coon⁽¹⁶⁾, and Conner.⁽¹⁷⁾ It was further extended to 20.0 MeV to pass evenly through the data points of Peterson⁽¹⁸⁻¹⁹⁾ between 17.3 and 28.8 MeV. The spline fits in the energy ranges 1-5 MeV and 5-20 MeV along with the experimental data are shown in Figs. 4 and 5, respectively.

(2) Elastic Cross Section

Because of the paucity of elastic scattering measurements, this cross section was derived by subtracting the non-elastic cross section from the total cross section. The non-elastic cross section is derived from the experimental data of Ref. 20-27 and is shown in Fig. 6. The sum of the various reactions (n,γ) , (n,n') , $(n,2n)$, $(n,3n)$, (n,p) , (n,α) , etc. is made equal to the non-elastic cross section.

(3) Capture Cross Section

The capture cross section below 2 keV is represented by the resonance parameters. In the energy region, 2-10 keV, the capture cross section was calculated by using the average resonance parameters specified previously and the code AVRAGE-4⁽²⁸⁾ which follows the method of Lane and Lynn⁽²⁹⁾ and applies width fluctuation corrections as discussed in their paper. (Fig. 7) (The curve between 10 keV and 20 keV is the same as that of Fig. 10.)

For neutron energies greater than 25 keV, a reassessment of the gold capture cross section is required because of the availability of new measurements and because of a reevaluation of the ^{235}U cross section for ENDF/B-IV. Fig. 8 shows the new ^{235}U fission cross section between 25 and 100 keV. It can be immediately seen that there is considerable structure in this cross

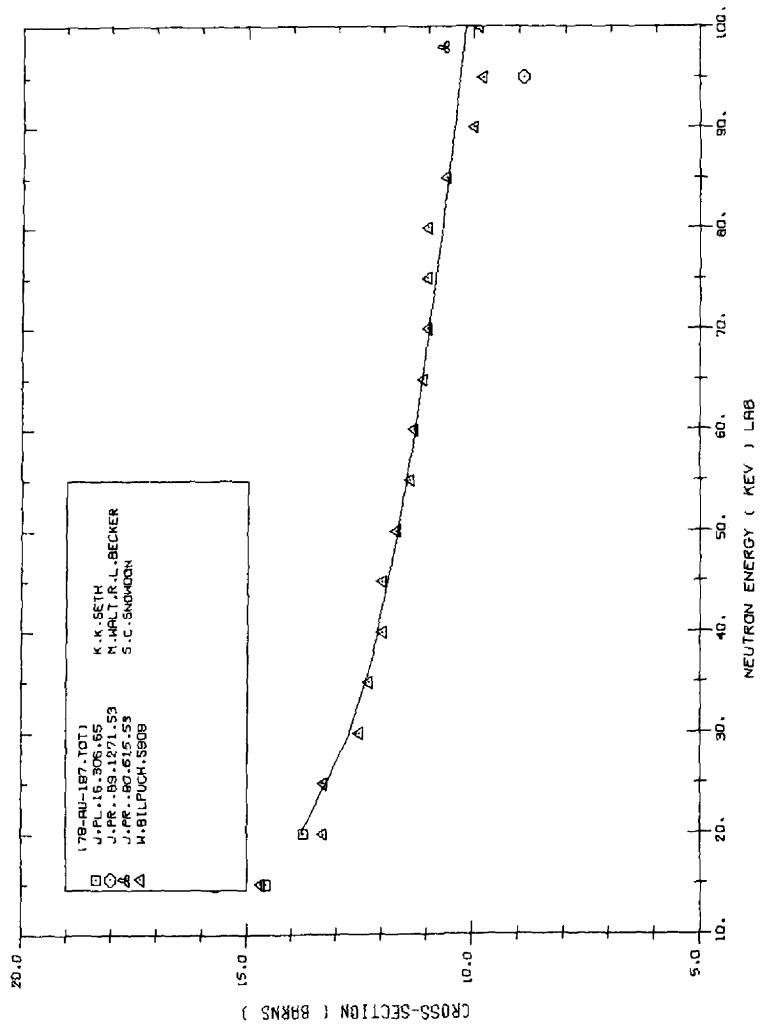


Figure 2. Total Cross Section 10-100 keV.

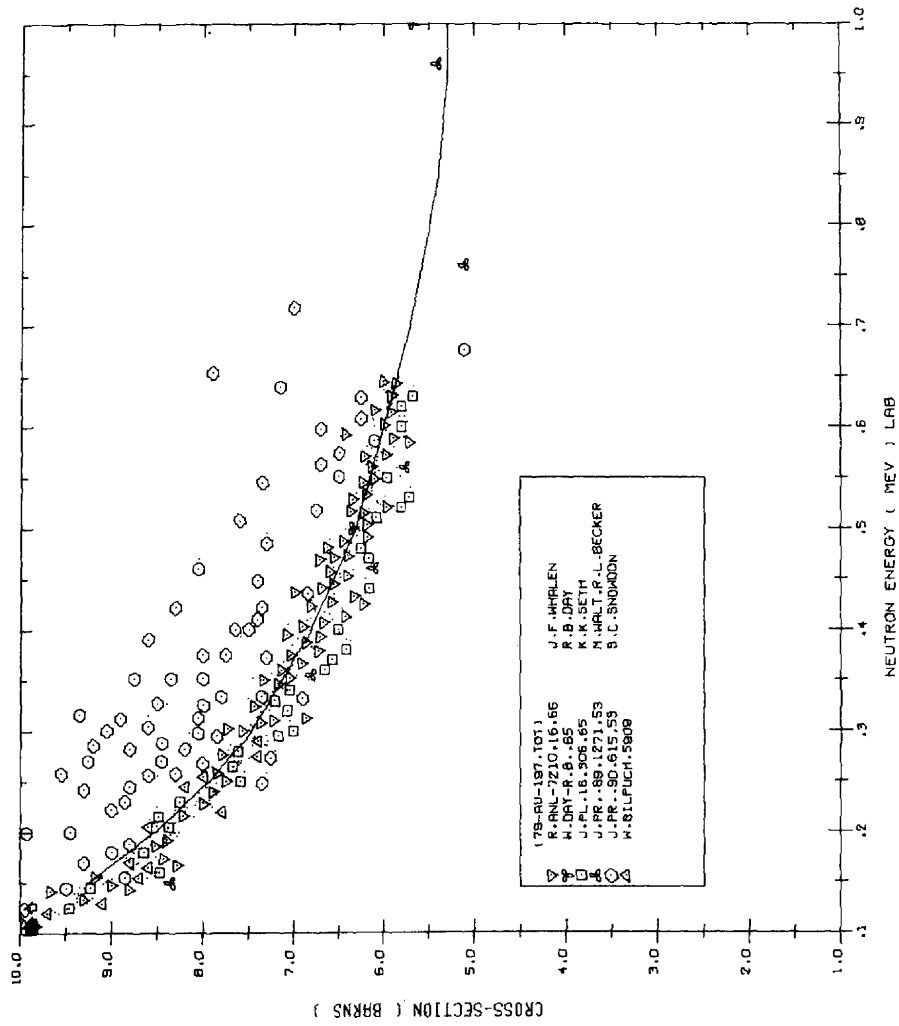


Figure 3. Total Cross Section 0.10-1.0 MeV.

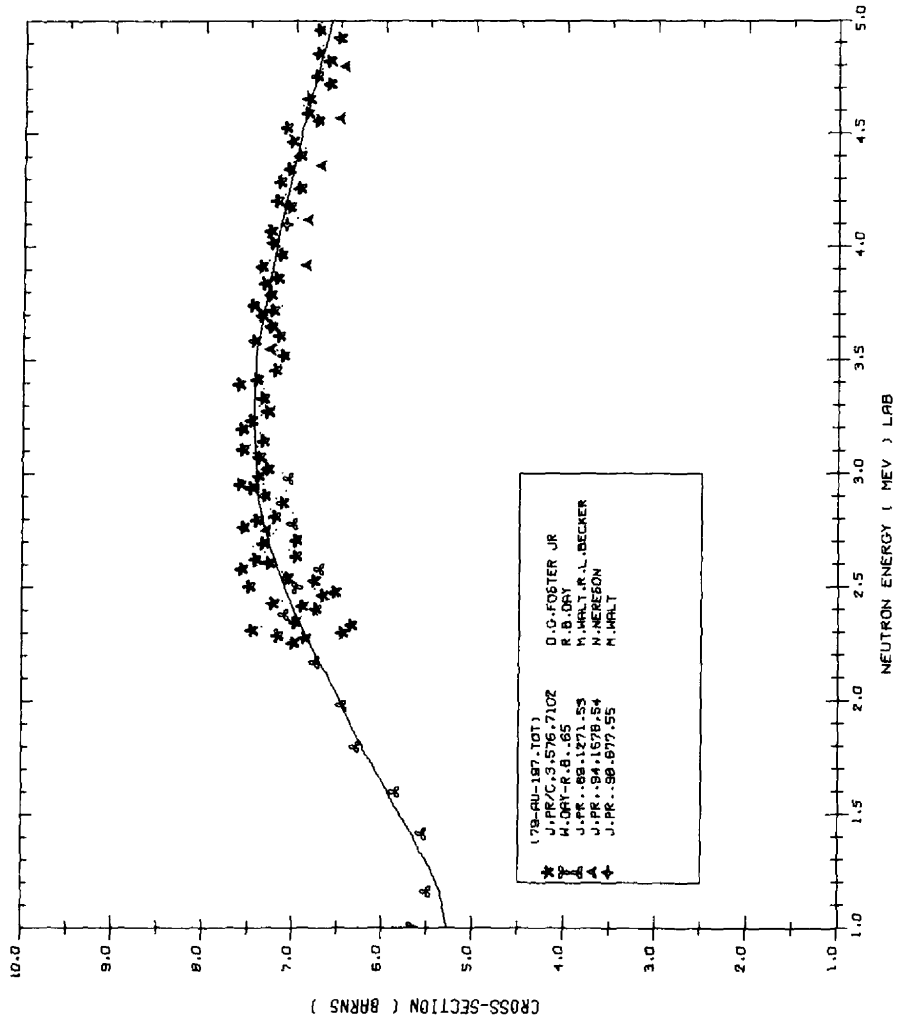


Figure 4. Total Cross Section 1.0-5.0 MeV.

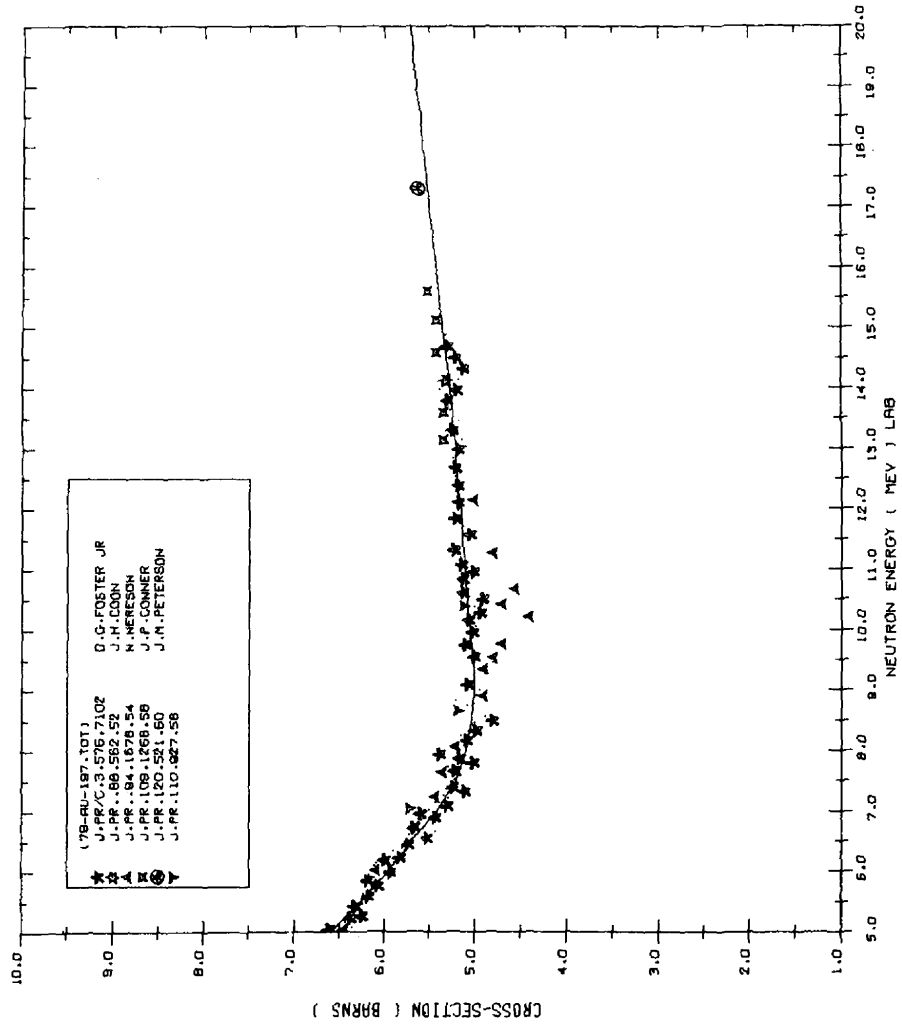


Figure 5. Total Cross Section 5.0-20.0 MeV.

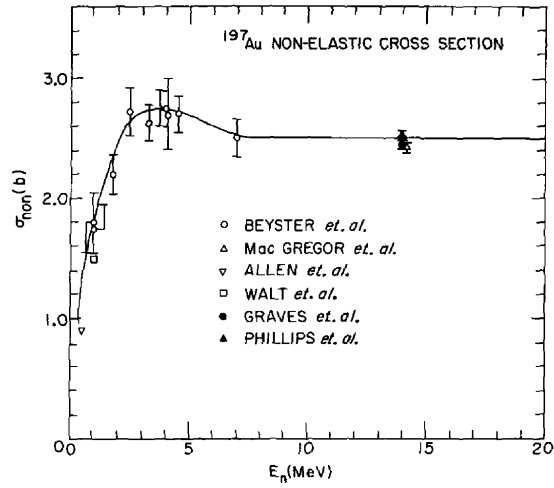


Figure 6. Non-Elastic Cross Section 0-20 MeV.

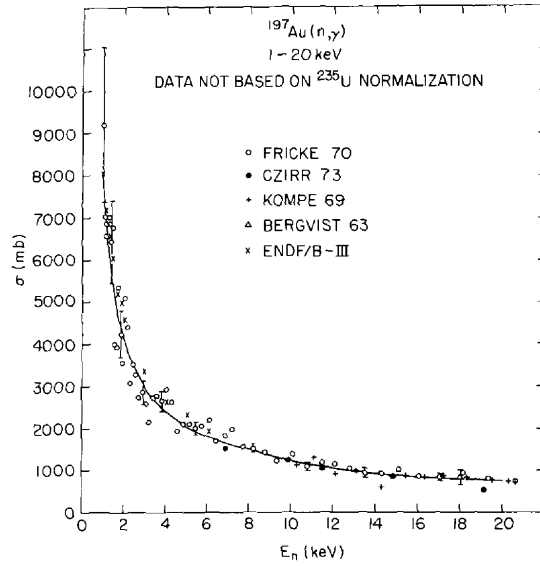


Figure 7. Capture Cross Section 1-20 keV.

section, with fluctuations of as much as 10% or more within a kilovolt or so. Thus, its use as a standard is quite compromised unless the neutron energy and neutron energy spread are well known and accounted for. In Fig. 9 this cross section is "smeared out" by averaging points in groups of ten (effective "resolution" ~ 5 keV) and compared to a similar curve for the ^{235}U fission cross section in ENDF/B-III. This plot indicates an average change in the absolute value of the cross section of 5-15%.

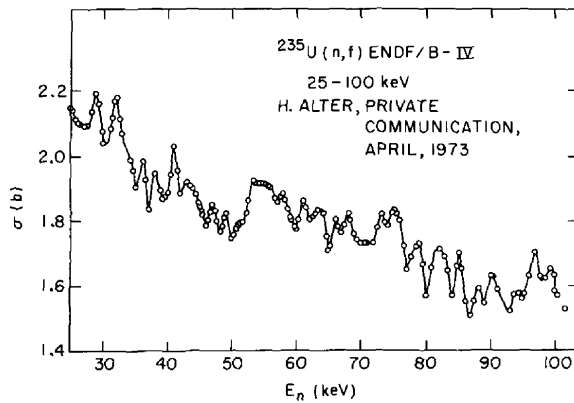


Figure 8. ^{235}U fission Cross Section 25-100 keV.

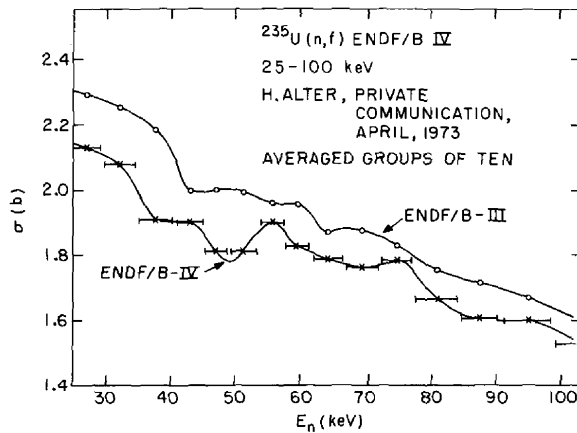


Figure 9. Averaged ^{235}U fission Cross Section 25-100 keV.

Since it would seem that a fluctuating cross section subject to substantial renormalizations, does not make a very reliable standard, it was decided to perform the gold capture re-evaluation with data not involving ^{235}U fission standardization. This follows the procedure adopted by Carlson⁽³¹⁾ and by Poenitz⁽³²⁾ in evaluations presented at the 1970 EANDC Normalization and Standards Conference held at Argonne National Laboratory and follows the most recent recommendations of the Normalization and Standards Subcommittee of CSEWG (July 1973). Due to an abundance of excellent recent experiments, it was also arbitrarily decided that only data measured since 1960 would be considered.

The capture cross between 10-100 keV is shown in Fig. 10. The following data sets were plotted: (1) Czirr et al⁽³³⁾ (2) LeRigoleur et al⁽³⁴⁾

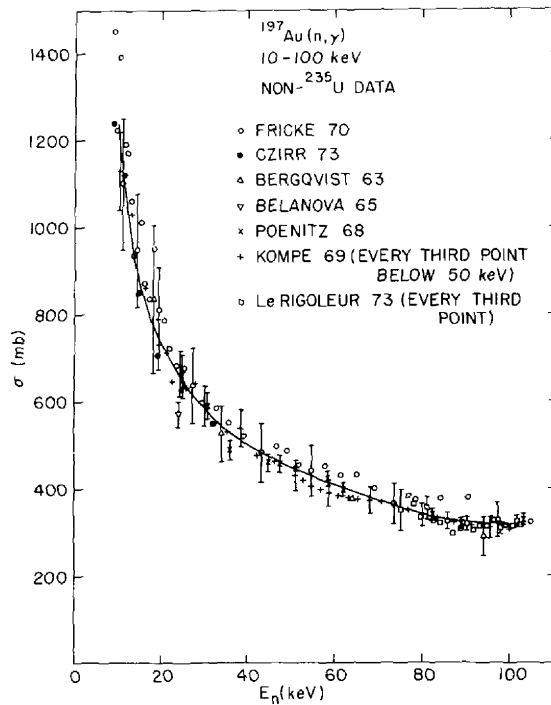


Figure 10. Capture Cross Section 10-100 keV.

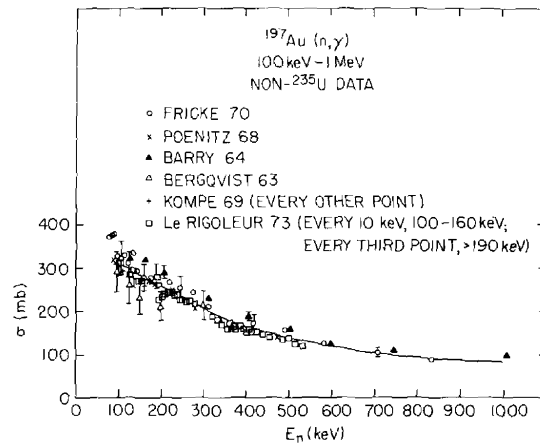


Figure 11. Capture Cross Section 100 keV-1MeV.

(3) Fricke et al⁽³⁵⁾ (4) Kompe⁽³⁶⁾ (5) Poenitz et al⁽³⁷⁾ (6) Belanova et al⁽³⁸⁾ (7) and Bergvist.⁽³⁹⁾ The data of Spitz et al⁽⁴⁰⁾ Moxon et al⁽⁴¹⁾ and Bilpuch et al⁽⁴²⁾ were not used.

The capture cross section between 100-1000 keV is shown in Fig. 11. Data sets of Refs. 34-38 were plotted, plus the data sets of Barry.⁽⁴³⁾

Inspection of Figs. 10 and 11 show that the various data sets are in quite good agreement with each other within the quoted errors. There is a general tendency for the data of Frick et al⁽³⁵⁾ (Fig. 10) and Barry⁽⁴³⁾ (Fig. 11) to be higher than others and for the data of Bergvist⁽³⁹⁾ to be lower; but all are never more than about two standard deviations from the mean. The one point of Belanova et al⁽³⁸⁾ is about three standard deviations low. The evaluated eye-guide in Figs. 10 and 11 was drawn with no explicit weight factors for the various experiments.

For the region above 1 MeV, there is only one significant new contribution, that of Lindner.⁽⁴⁴⁾ These data should be considered preliminary until published and were measured relative to ²³⁵U, but the lack of measured fluctuations in the ²³⁵U fission cross section at these high energies made it worthwhile to

see what the new data indicated for gold capture. Fig. 12 shows two independently normalized data sets from Lindner⁽⁴⁴⁾ between 0.5 and 3 MeV. The curve between 0.5 and 1 MeV is that of Fig. 11 and above 1 MeV is that of ENDF/B-III. The data up to 2.2 MeV are in excellent agreement with the old evaluation. The two higher energy points are low by about 15% and 20% respectively. It was felt that it was not worthwhile to give these points sufficient weight to seriously distort the ENDF/B-III curve, which represents the best curve through all previous measurements. An added inducement for not trying a serious reassessment of all of the data above 1 MeV was the implications of the effect noted by Devaney.⁽⁴⁵⁾ Devaney points to the importance of a multiple reactions correction for reaction cross section measurements above approximately 100 keV. The correction is particularly important for radiative capture, even with fairly thin samples. The relevance of this effect to specific gold capture experiments is unknown, but should be determined before the higher energy gold capture data are reevaluated again.

In conclusion, the evaluated curve of ENDF/B-III between 1 and 20 MeV, which included the evaluation of Vaughn and Grench⁽⁴⁶⁾ (1.0 - 5.2 MeV) and that of Bogart⁽⁴⁷⁾ above 5.2 MeV, are adopted for ENDF/B-IV.

It is of interest to calculate the fission spectrum averages of the capture and other reaction cross sections and compare them with experimental

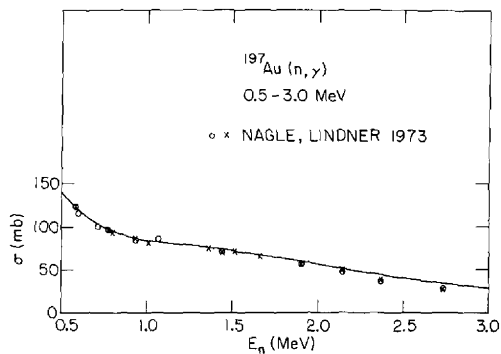


Figure 12. Capture Cross Section 0.5-3.0 MeV.

measurements. For this purpose, a Maxwellian ^{252}Cf fission spectrum of characteristic temperature 1.39 MeV and represented by

$$\phi(E) = C \sqrt{E} e^{-\frac{E}{T}}$$

was used. (C is a normalizing constant.) The calculated fission spectrum average of the ENDF/B-IV (n, γ) reaction of gold is 81.8 mb. This number is to be compared with an experimental value of 95.5 ± 2.3 mb measured by Pauw and Atin.⁽⁴⁸⁾ Since the capture cross section in the whole energy range 0.100-1.5 MeV is believed to be known to better than 18%, the source of this discrepancy could be due to either the measurement and/or the inadequacy of representing the fission spectrum by a Maxwellian form at low energies. The ^{235}U fission spectrum average measurements of Fabry⁽⁴⁹⁾ shed some light on the former explanation. Fabry obtains a value of 88.0 ± 4.5 mb for $^{197}\text{Au}(n,\gamma)$ ^{198}Au reaction. With a characteristic temperature $T = 1.29$ MeV for ^{235}U , we obtain a fission spectrum average of 86.4 mb which is within the stated error of Fabry.⁽⁴⁹⁾

After the completion of the evaluation of the capture cross section of Au, it was found that two points had been inadvertently omitted from consideration. Both were measured with the same technique at the National Physical Laboratory in England. At 25 keV, Ryves et al⁽⁵⁰⁾ measured a value of 640 ± 25 mb. This is in excellent agreement with the value of 648 mb read from Fig. 10. At 966 keV, Robertson et al⁽⁵¹⁾ measured a value of 96.2 ± 2.0 mb. This value is approximately 12% higher than the value at this energy from Fig. 11. No changes were made as a result of this discrepancy for the reasons noted above regarding the Devaney⁽⁴⁵⁾ multiple reaction correction effect. In addition the following data sets become available at the time of the writing of the report:

- (1) Poentiz⁽⁵²⁾ data in the energy range 400 - 3500 keV. This is an absolute measurement carried out by a large liquid scintillator for the detection

of prompt capture gamma rays. The Grey Neutron Detector, the Black Neutron Detector and a ^6Li -glass detector were employed to measure and monitor the neutron flux.

- (2) Macklin et al⁽⁵⁾ data in the energy range from 3 to 550 keV. In this measurement a scintillation detector and a ^6Li neutron monitor were used. The efficiency of the detector was normalized to the 4.9 eV gold resonance by the saturation method. The ^6Li neutron cross section of Uttley, slightly modified, was adopted.
- (3) Rimawi and Chrien⁽⁵³⁾, using the iron filtered beam, measured the neutron capture cross section of Gold at 24.5 keV by the activation method. Assuming a $^{10}\text{B}(n,\alpha\gamma)^7\text{Li}$ cross section of 3.487 b and a total reaction cross section of 5.9175 b for ^{10}B , a total capture cross section for ^{10}B of 0.630 ± 0.006 b is obtained. The error indicated is only statistical and does not include the uncertainty in the normalization. These new measurements were plotted and compared with the ENDF/B-IV capture cross section in the pertinent energy regions. Good agreement is noted between the new measurements and the evaluated ENDF/B IV capture cross section.

Finally, it may be noted that preliminary results of the capture cross section of gold between 100 keV and 500 keV were reported by Forte⁽⁵⁴⁾ in a progress report. A $4\pi\beta\gamma$ detector was used to detect the induced activities. The data is not yet available. Fort made, however, a comparison between his data and those of Rigoleur and stated that there is reasonable agreement between the two measurements. These new data sets will be considered in the evaluation of the $\text{Au}(n,\gamma)$ cross-section for ENDF/B-V.

4. Inelastic Scattering Cross Section

The inelastic scattering cross section data of DeVilliers et al⁽⁵⁵⁾ and Barnard et al⁽⁵⁶⁾ were considered. The latter authors reported data in a neutron energy region closer to threshold than was previously measured. The

experimental data extended only to an energy of 1.6 MeV. The techniques, normalizations and corrections applied by both of these groups are similar. Corrections for neutrons scattered inelastically after an initial elastic scattering event in the Au sample were applied by using the Monte Carlo method. Detector efficiency was determined by normalizing to the carbon cross sections as given by Langsdorf et al.⁽⁵⁷⁾ The scattered neutron energy resolution of both experiments was about 20 keV. Because of this limitation, many observed inelastic peaks were not resolved, such as the 268 and 279 keV level. Angular distributions of inelastic neutrons were measured for the 77 keV and the combined (268 + 279) keV levels. These were found to be isotropic within the statistical and experimental errors, which were of the order of 10%. The data of Barnard et al.⁽⁵⁶⁾ and DeVilliers et al.⁽⁵⁵⁾ are in reasonable agreement with each other within the stated errors.

In addition, Nelson et al.⁽⁵⁸⁾ measured the gamma ray differential production cross sections below 1308 keV excitation energies using a GeLi detector. These authors reported accurate energies for the observed γ rays from which they constructed an energy level diagram for ^{197}Au . This was useful in assessing the pertinent data on the level diagram of ^{197}Au .

In the neutron energy region where experimental information is not available, i.e., near threshold and above $E_n = 1.6$ MeV, the evaluation is based on a properly normalized statistical model calculations following the formalism of Hauser and Feshbach. In order to carry out these calculations, a knowledge of the spins and parities of the ^{197}Au levels are required. The model calculations were carried out with the aid of the code COMNUC 1,⁽⁵⁹⁾ using basically the level diagram scheme of ^{197}Au as reported by the Nuclear Data Group⁽⁶⁰⁾ and Barnard et al.⁽⁶¹⁾ (Fig. 13). Inelastic scattering cross section to the continuum of levels and specified by a low energy cut off of 1.25 MeV is obtained by using COMNUC 1. The derived values are normalized to the difference between non-elastic and the sum of discrete inelastic and (n, particle) reaction cross sections.

Figs. 14 - 22 summarize the experimental inelastic scattering cross section data and presents the evaluated curves in the energy range from threshold to 3.0 MeV. In the evaluated files, the inelastic cross sections exciting the individual levels are given. However, for the purpose of comparison with the experimental data where levels are not resolved, the sum of the pertinent inelastic cross sections is presented here, for example the 268 and 279 keV levels.

5. (n, particle) Cross Sections

No significant data have been published recently. The second supplement⁽¹⁾ to the second edition of BNL-325 provides an adequate summary. Most new measurements of the (n, particle) reactions are concerned with the emission spectra and explanation in terms of the pre-equilibrium model. Only the (n, 2n), (n, 3n), (n,p), and (n, α) reactions are described. Other

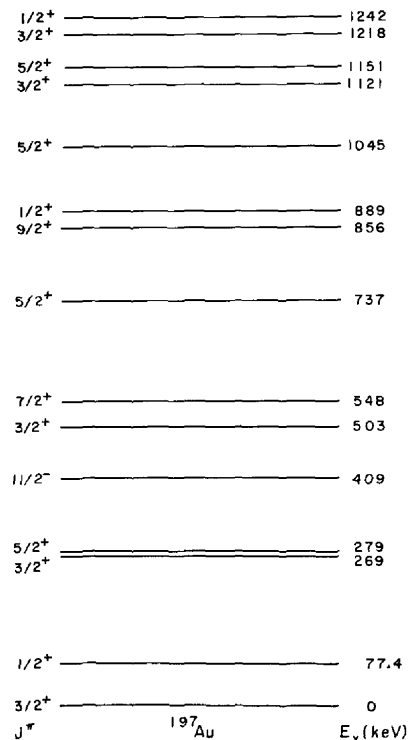


Figure 13. Energy Levels of ^{197}Au .

particle reactions such as (n, t) reactions are energetically possible but experimental data are scant. Q values are based on the Wapstra and Gove⁽⁶²⁾ 1971 tables.

(a) (n, 2n) Cross Section

The Q value is -8.078 MeV. Data are provided for the formation of the ¹⁹⁶Au 6.2 day ground state and the 10 hour metastable (the sixth level) state. The partial cross sections must be summed to yield the total ¹⁹⁷Au (n, 2n) ¹⁹⁶Au cross section. Below 12 MeV the data of Tewes et al⁽⁶³⁾ are recommended. From 12 to 20 MeV, the recommended values are based on the data of Prestwood and Bayhurst⁽⁶⁴⁾ Dilge⁽⁶⁵⁾, Qaim⁽⁶⁶⁾, Hankla et al⁽⁶⁷⁾, Nethaway⁽⁶⁸⁾, and Mather.⁽⁶⁹⁾ Recent measurements of Liskien⁽⁷⁰⁾ have not been released in published form. Fig. 23 describes the experimental data and presents the evaluated ENDF/B IV (n, 2n) cross section and compares it with previous evaluation. The evaluation proceeded along the following lines:

Cross section values were chosen for production of the isomeric state which was about 0.1 of the ground state production cross section. This is specified in the files. (MAT 26.) A peak total (n, 2n) cross section of 2.15 barns was derived based on a nonelastic cross section of $2.45 \pm .03$ barns (Fig. 6) and charged particle emission cross sections of a few tens of millibarns.

The calculated (n, 2n) cross section (T = 1.39 MeV) averaged over a ²⁵²Cf fission spectrum is 5.11 mb. This is in good agreement with an experimental value⁽⁴⁸⁾ of 4.93 ± 0.14 mb. The overall data uncertainty is estimated to be 20%.

(b) (n, 3n) Cross Section

Only one measurement, at 14.4 ± 0.4 MeV, is reported⁽⁶⁷⁾ in the literature for the (n, 3n) reaction of ¹⁹⁷Au ($\sigma = 61 \pm 20$ mb). The threshold is taken at 14.747 MeV and the (n, 3n) cross section curve is determined essentially by subtraction of the nonelastic and the (n, 2n) cross sections

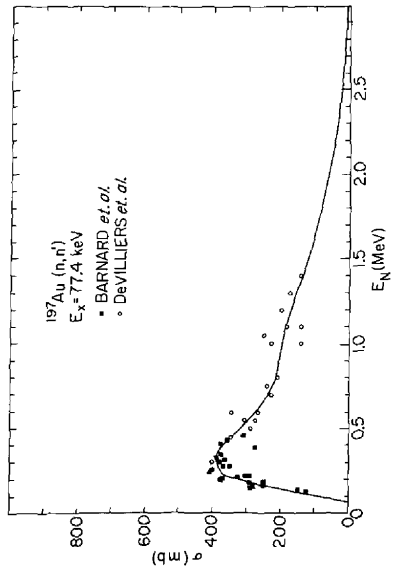


Figure 14. Inelastic Cross Section exciting the 77.4 keV level.

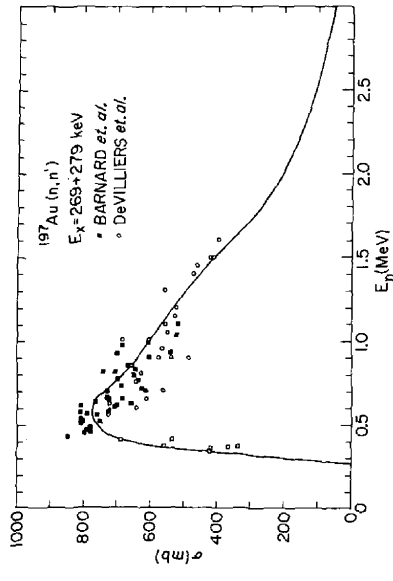


Figure 15. Inelastic Cross Section exciting the combined levels at 269 and 279 keV.

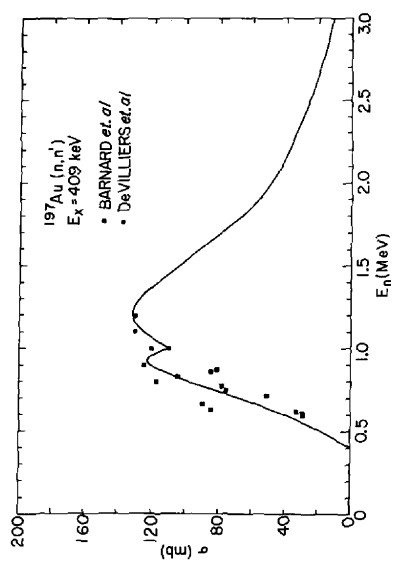


Figure 16. Inelastic Cross Section exciting the 409 keV level.

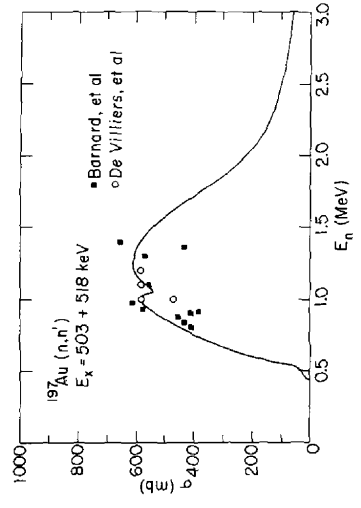


Figure 17. Inelastic Cross Section exciting the combined levels at 503 and 518 keV.

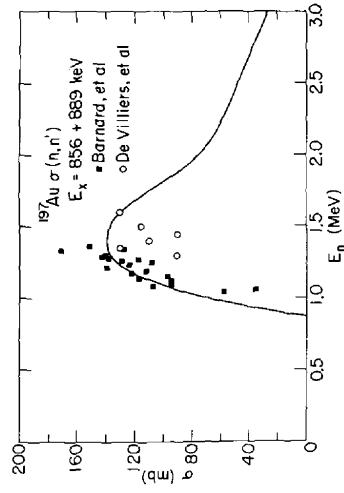


Figure 18. Inelastic Cross Section exciting the level at 737 keV.

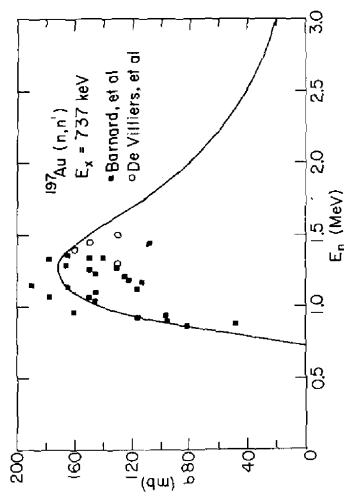


Figure 19. Inelastic Cross Section exciting the combined levels at 856 and 889 keV.

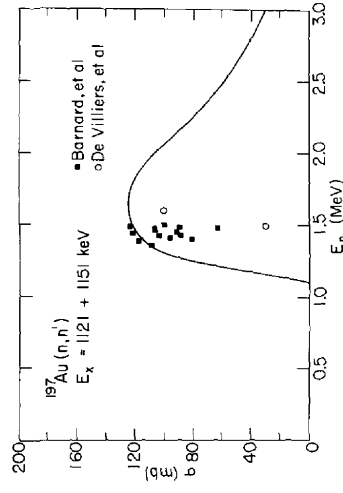


Figure 20. Inelastic Cross Section exciting the 1045 keV level.

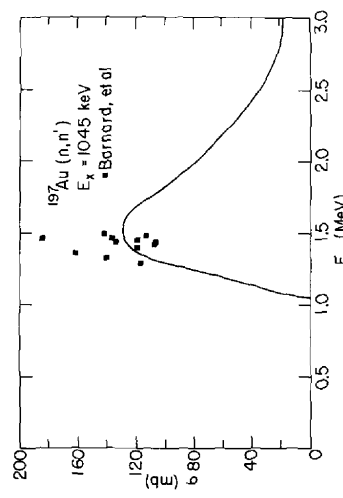


Figure 21. Inelastic Cross Section exciting the combined levels at 1121 and 1151 keV.

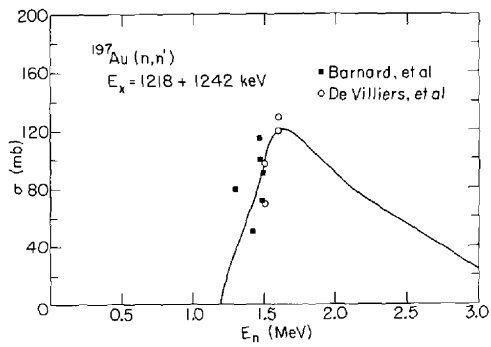


Figure 22. Inelastic Cross Section exciting the combined levels at 1218 and 1242 keV.

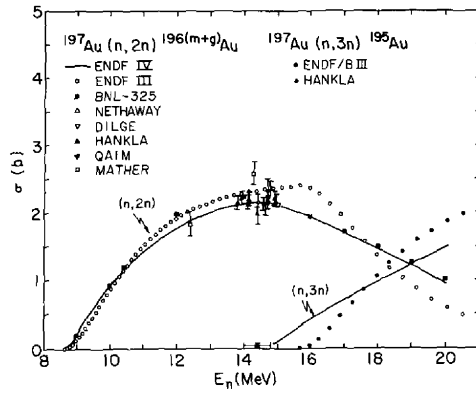


Figure 23. The (n,2n) and (n,3n) Cross Sections.

from the total cross section. Fig. 23 shows the evaluated (n, 3n) cross section and compares it with previous evaluation.

(c) (n,p) Cross Section

The Q value is -0.036 MeV. The recommended values follow the data of Bayhurst and Prestwood⁽⁷¹⁾ through the entire energy range. Fig. 24 presents the (n, p) cross section; also included in the Fig. is the datum point of Coleman et al⁽⁷²⁾ which is in line with the data of Bayhurst and Prestwood.⁽⁷¹⁾ These data are ignored and an overall uncertainty of 25% is estimated for the evaluation. The calculated ²⁵²Cf fission spectrum averaged cross section is 2.37 μ b. No experimental data is available to compare this calculation.

(d) (n, α) Cross Section

The Q value is -6.964 MeV. The data of Bayhurst and Prestwood⁽⁷¹⁾ determine the evaluated cross section which is shown in Fig. 25. Note that at $E_n = 14.5$ MeV Bayhurst and Prestwood and Coleman et al determined by the activation method an (n, α) cross section of 0.37 ± 0.02 mb, and 0.43 ± 0.04 mb respectively. An overall uncertainty of 20% is assigned to the evaluation. It is of interest to point out that Marcazzan et al⁽⁷³⁾ determined a differential (n, α) cross section at 30° of $0.70 \pm .03$ mb/steradian and reported a forward peaking in the α particle emission. Specifically, the ratio of the number of α particles emitted in the forward and backward directions was found to be approximately 5. Comparison of the energy spectra of α particles measured by Marcazzan et al⁽⁷³⁾ at 30° with those of Kitazawa⁽⁷⁴⁾ at 0° seem to confirm this forward peaking in the α particle emission, hence indicating direct reaction contribution. Further experimental and theoretical studies are required to fully understand this reaction mechanism. It seems that the statistical model description of the (n, α) reaction is not in complete accord with these findings.

The calculated ²⁵²Cf fission spectrum averaged cross section is 0.76 μ b.

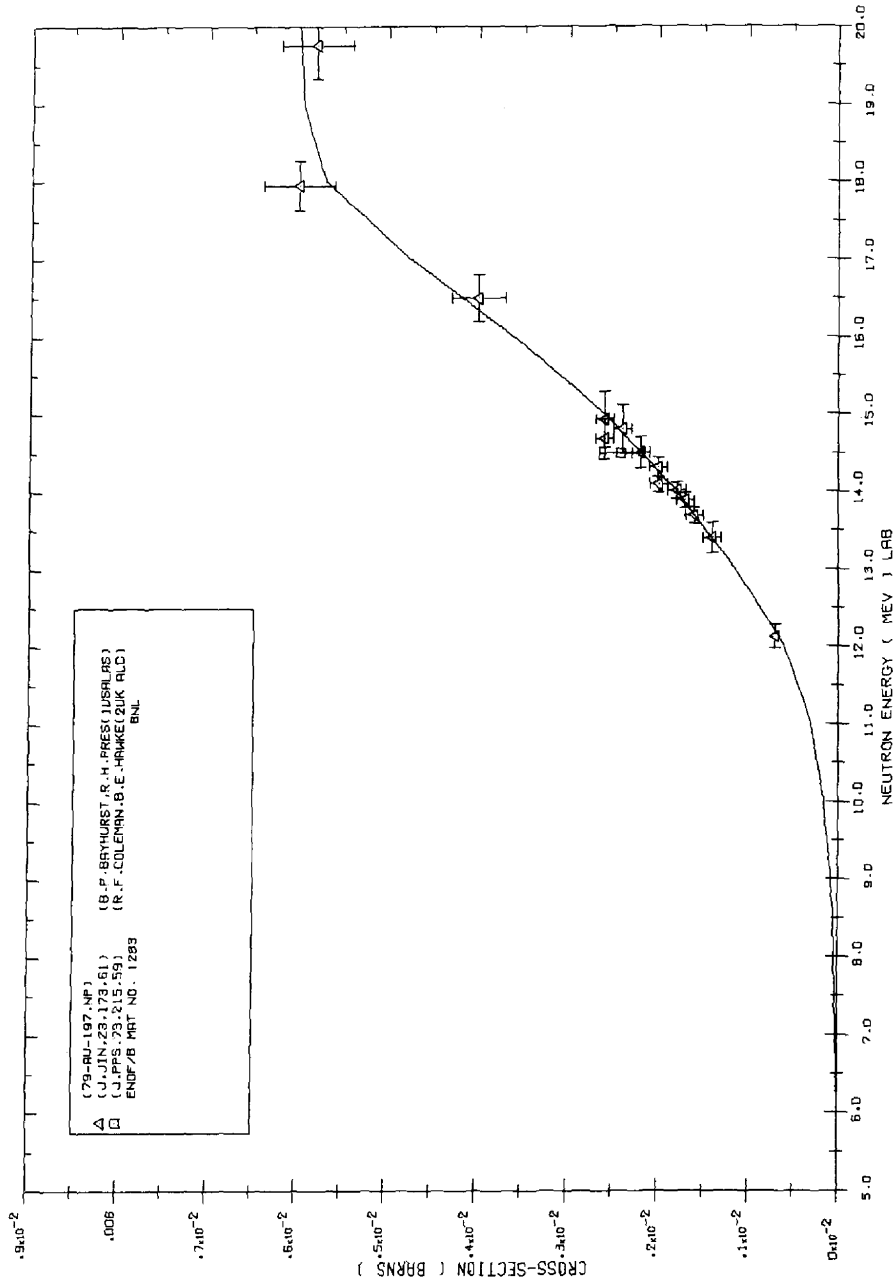


Figure 24. The (n,p) Cross Section.

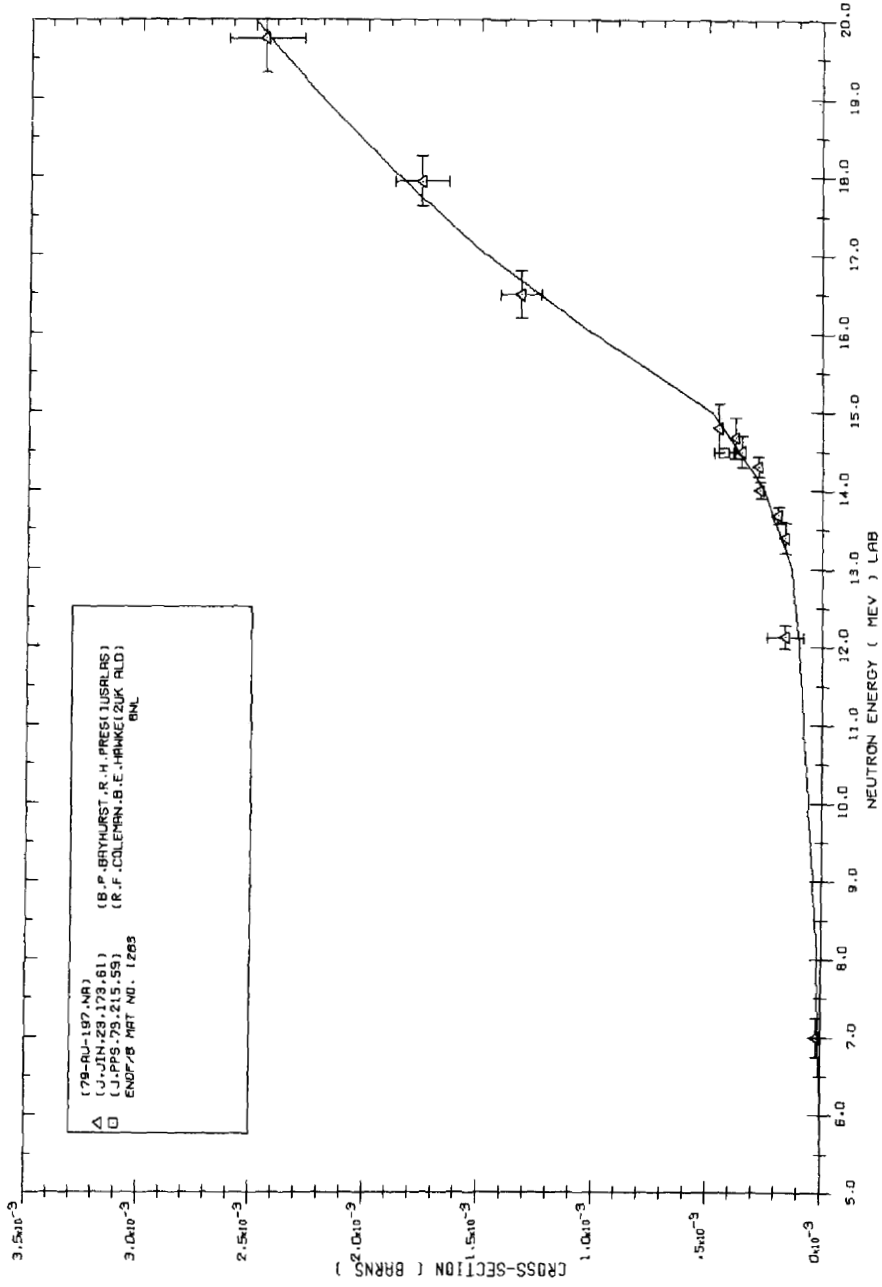


Figure 25. The (n,α) Cross Section.

IV. Angular Distribution of Secondary Neutrons

The elastic scattering angular distribution in the energy range up to 8.05 MeV are based on the following experimental data:

- (a) Holmqvist and Wiedling⁽⁷⁵⁾
- (b) Buccino et al⁽⁷⁶⁾
- (c) Kuchnir et al⁽⁷⁷⁾
- (d) Allen et al⁽²⁷⁾
- (e) Walt and Beyster⁽⁷⁸⁾
- (f) Walt and Barshall⁽⁷⁹⁾
- (g) DeVilliers et al⁽⁵⁵⁾

With the aid of the optical model parameters derived by Holmqvist and Wiedling⁽⁷⁵⁾, optical model calculations were carried out by using ABACUS-2.⁽⁸⁰⁾ The calculations were compared with measurements at the following neutron energies; 0.5, 1.0, 2.0, 2.5, 5.0, and 8.05 MeV. The agreement between calculations and measurements is reasonably good, enough to warrant extrapolating the calculations above 8.1 MeV where experimental data are not available. In addition, the graphic display code TIGER (ref. 81) was utilized to fit the experimental data with a least-squares spline procedure, check Wick's limit, and then extract Legendre coefficients of various orders for the angular distribution of scattered neutrons. Figs. 26 - 29 present the results of the least-squares for neutron energies 0.5, 1.0, 2.0, and 5.0 MeV and compare them with the experimental data.

There are no complete systematic investigation of the angular distribution of reactions in ^{197}Au . The forward peaking in the (n, α) emission of ^{197}Au was pointed out previously. Measurements on other heavy nuclei at 14 MeV indicate non-isotropic distributions but not appreciably symmetric about 90° . This reflects the fact that direct reaction contribution plays an important role.

E IN 5.0000E+05 EV
(79-AU-197,EL,DA)

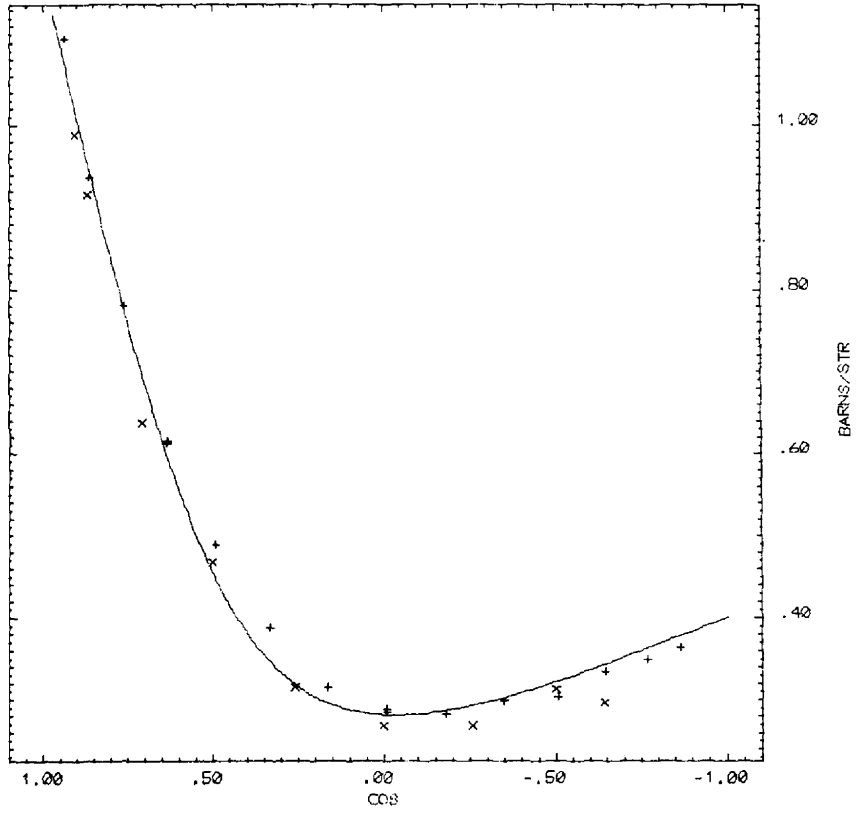


Figure 26. Elastic Angular Distribution for En=0.5 MeV.

E IN 1.0000E+06 EV
(79-AU-197,EL DA)

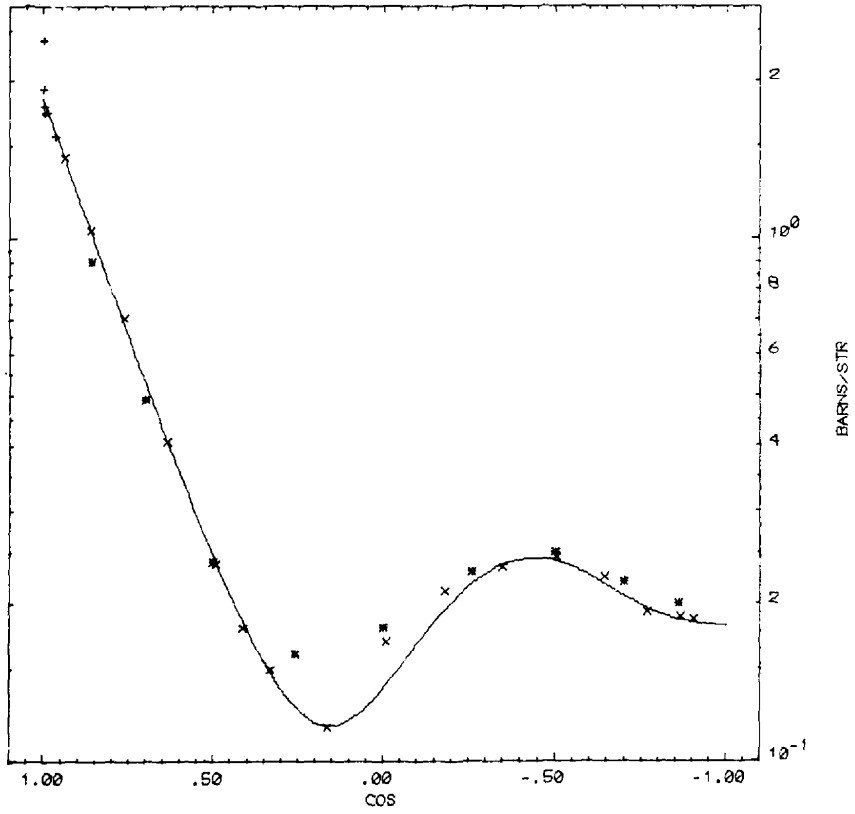


Figure 27. Elastic Angular Distribution for En=1.0 MeV.

E IN 2.500E+06 EV
(79-AL-197, EL DA)

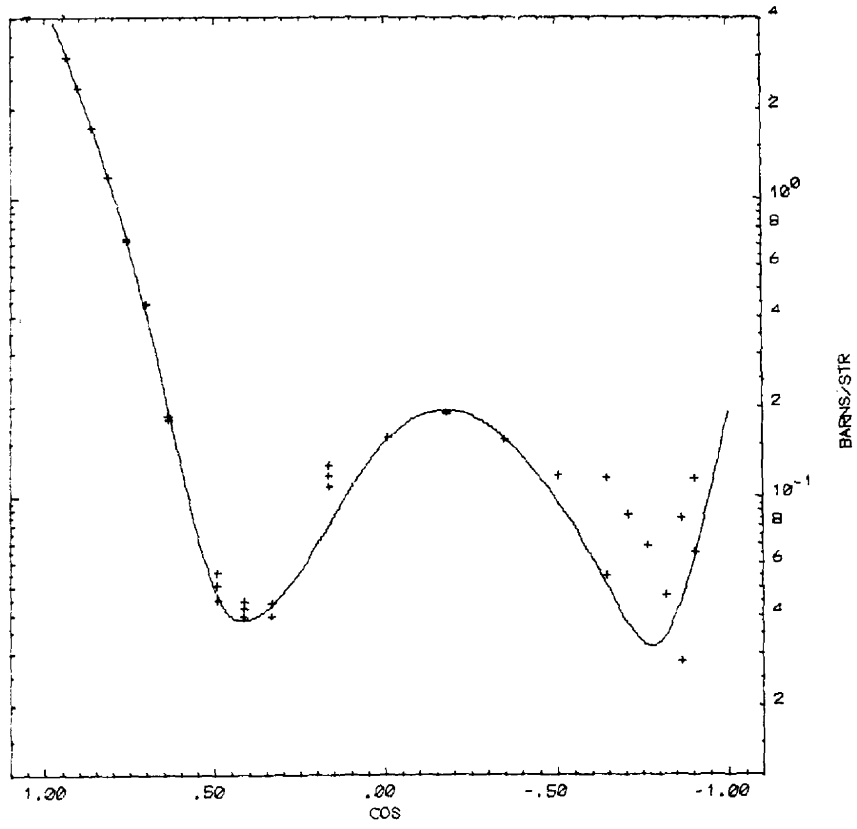


Figure 28. Elastic Angular Distribution for $E_n=2.5$ MeV.

E IN 5.0000E+06 EV
(79-AU-197, EL D4)

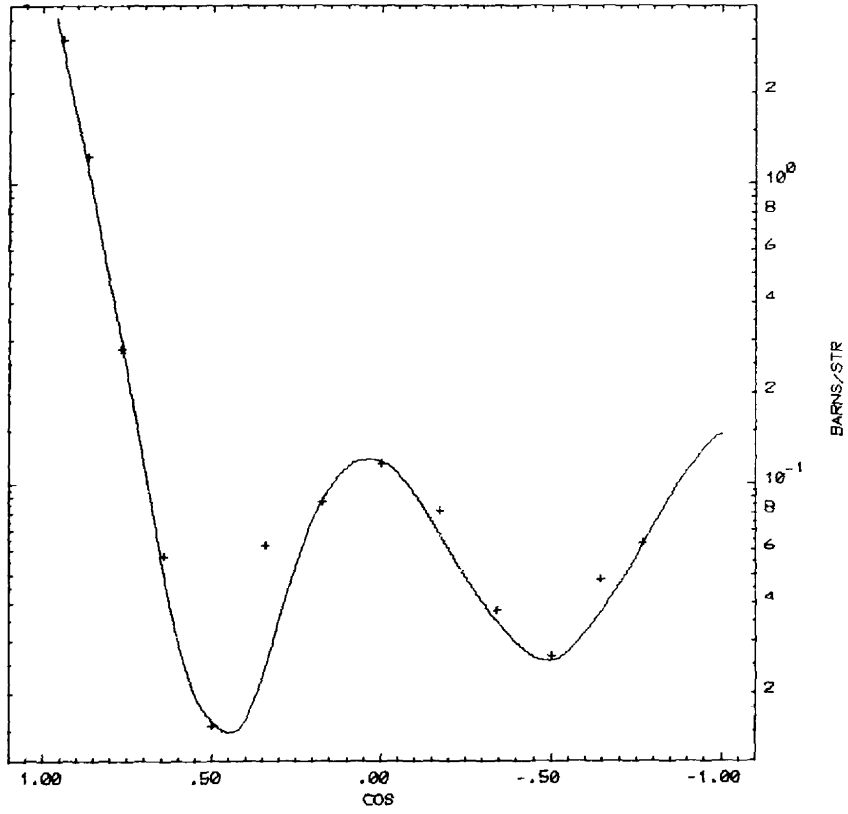


Figure 29. Elastic Angular Distribution for En=5.0 MeV.

In this evaluation, the angular distribution for the (n, particle) reactions have been specified as isotropic.

V. Energy Distribution of Secondary Neutrons

The energy spectra of the emitted particles are considered to consist of two parts: an evaporation spectrum peaking at a characteristic temperature, T , and a high energy component resulting from direct or pre-equilibrium processes. The spectral data presented in this evaluation whether presented in parametric or tabulated form were derived on the basis of the forgoing models.

The nuclear temperatures for the evaporation process were obtained from inelastic scattering data of Anufrienko⁽⁸⁴⁾ taken over a large range of incident and emerging energies. For a given incident energy, data for high energy emergent particle (single particle emission) are extrapolated to lower energies and subtracted from the total data to determine evaporation spectra and nuclear temperatures.

For $A > 100$, T is generally constant except near magic number nuclei. Nuclear temperatures for tungsten⁽⁸⁴⁾ were adopted here.

The pre-equilibrium model⁽⁸⁵⁾, with some approximations, was used to represent the high energy spectra. The fraction of pre-equilibrium contribution to the total emission spectra is approximately linear with energy in the case of Nb.⁽⁶⁾ This assumption roughly holds for other cases.⁽⁸⁷⁾ There is a slow variation with mass, about $A^{1/3}$, for the pre-equilibrium cross section to be compared with an A dependence of the evaporation cross section. For Au, the fraction of pre-equilibrium emission to the total is about 0.28⁽⁸⁷⁾ at an excitation energy of 28 MeV. In this evaluation, the spectra were calculated according to the following prescription.

$$N(E) = P(E) \left\{ (1-f) E e^{-\frac{E}{T}} + f E \sum_{\substack{\bar{n} \\ n_0 \\ \Delta n \neq 2}} \left(\frac{E_n - E}{E_n + B} \right)^{n-2} n(n-1) \right\}$$

T = nuclear temperature

$$n_0 = 3$$

$$\bar{n} = \sqrt{2aE_n}$$

a = nuclear level density

E_n = incident energy

B = binding energy (in lab)

f = fraction pre-equilibrium

P(E) = coulomb barrier penetrability

The use of P(E) is an approximation to the usual statistical formula that would ordinarily include the inverse cross section for capture of the emerging particle. For simplicity, the same T and f energy dependence was assumed for all reactions with final spectra greatly influenced by the coulomb barrier and Q values.

VI. Summary and Conclusion

The total, capture, and scattering cross sections of gold below 2 keV are represented by single-level Breit-Wigner parameters. Because of the presence of strong resonances, which resulted in strong interference effects, the scattering and total cross sections became negative at a few energy points. To remedy this unacceptable behavior, a background cross section was included in the file. Therefore, it is recommended that in future evaluations, a multilevel formalism be utilized. Since the parameters of a bound level were derived, the need to add a 1/V term to describe the cross section at low energies was eliminated. The absorption resonance integral calculated from the resonance parameters and from the unresolved and

high energy region is in excellent agreement with the recommended value which is based on the experimental data.

The capture cross section at 2200 m/sec ($\sigma_{\gamma} = 98.8 \pm 0.3b$) is one of the best known capture cross sections and as a result provides an excellent standard for other capture cross section measurements. Recent determination by Dilge et al⁽⁸⁸⁾ provides further confirmation of this fact. An absorption cross section of $98.68 \pm 0.12b$ was obtained by Dilge et al⁽⁸⁸⁾ by a precision total cross section measurement in the 40 μ eV - 5 meV energy range. Because of the presence of structure in the capture cross section of gold in the unresolved energy range, care must be exercised in the use of gold as a standard, as pointed out by Macklin et al.⁽⁵⁾ At higher energies and below about 500 keV, the capture cross section is presently known to an accuracy of better than 5%.

The total cross section above 2 keV is represented by a spline fit to the experimental data. In the energy range above 100 keV and neglecting the Snowdon data⁽¹²⁾, there is a spread of 10% - 15% in the experimental data. Because of the simplicity of total cross section measurements and in order to understand other cross sections to better accuracy, such as scattering cross sections, a precision measurement of the total cross section of gold is desirable.

The inelastic cross sections exciting discrete levels of ^{197}Au up to energies of 1242 keV are described. Experimental data are available only for a limited neutron energy region; ie.; below 1.6 MeV. At higher energies and very close to thresholds, the inelastic cross sections are represented by normalized Hauser-Feshbach calculations via COMNUC-1.

The (n, particle) reaction cross sections, (n, 2n), (n,p), (n, α) are evaluated with emphasis placed on the experimental data. It will be useful to include other particle reactions such as (n, t), (n, np) in future evaluations. Because of the presence of forward peaking in studies such as

(n, α) reactions, it is essential to abandon the use of isotropic angular distributions and replace them by the proper form. If experimental data is either scarce or not available on the pertinent nucleus, studies of neighboring nuclei may shed light on this aspect. Further experimental and theoretical studies of the systematics of this effect are required.

Acknowledgements

We would like to express our thanks to R.R. Kinsey and B.A. Magurno for their help in running some computer codes and to C. Brewster for the production of Figs. 24 and 25.

References

- (1) S.F. Mughabghab and D.I. Garber, Neutron Cross Sections, BNL 325, 3rd Edn., Vol. 1 (1973). See also M.D. Goldberg, S.F. Mughabghab, S.N. Purohit, B.A. Magurno, and V.M. May, BNL 325, Second Edition, Second Supplement, Vol. IIC (1966).
- (2) A. Lottin and A. Jain, Conference on Nuclear Structure with Neutrons, Budapest, 1972, p. 34 and private communication.
- (3) O.A. Wasson, R.E. Chrien, M.R. Bhat, M.A. Love, and M. Beer, Phys. Rev. 173, 1170 (1968).
- (4) E. Haddad, R.B. Walton, S.J. Friesenhahn and W.M. Lopez, Nucl. Inst. and Methods 31, 125 (1964).
- (5) R.L. Macklin, J. Halperin, and R.R. Winters, Private communication (1974). To be published in Phys. Rev.
- (6) G. Hacken, H.T. Liou, W. Makofske, F. Rahn, J. Rainwater, H.S. Camarda, and M. Slagowitz, Bull. Am. Phys. Soc. 18, 96 (1973).
- (7) K.K. Seth, Phys. Letters 16, 306 (1965).
- (8) E.G. Bilpuch, private communication ANISN 52315/6 (1959).
- (9) J.F. Whalen, ANL-7210, 16 (1966).
- (10) R.B. Day, private communication ANISN 520415/2 (1965).
- (11) M. Walt and R.L. Becker, Phys. Rev. 89, 1271 (1953).
- (12) S.C. Snowdon, Phys. Rev. 90, 615 (1953).
- (13) D.G. Foster Jr., private communication AN/SN 10047/86 (1967).
- (14) M. Walt, Phys. Rev. 98, 677 (1955).
- (15) N. Nerison, Phys. Rev. 94, 1678 (1954).
- (16) J.H. Coon, Phys. Rev. 88, 562 (1952).
- (17) J.P. Conner, Phys. Rev. 109, 1268 (1958).
- (18) J.M. Peterson, Phys. Rev. 110, 927 (1958).
- (19) J.M. Peterson, Phys. Rev. 120, 521 (1962).
- (20) J.R. Beyster, Phys. Rev. 98, 1216 (1955).
- (21) J.R. Beyster, Phys. Rev. 104, 1319 (1956).
- (22) M.H. Macgregor, Phys. Rev. 108, 726 (1957).
- (23) M. Walt, Phys. Rev. 93, 1062 (1954). See also Phys. Rev. 98, 677 (1955).

- (24) E.R. Graves, Phys. Rev. 89, 343 (1953).
- (25) E.R. Graves, Phys. Rev. 97, 1205 (1955).
- (26) D.D. Phillips, Phys. Rev. 88, 600 (1952).
- (27) R.C. Allen, R.W. Walton, R.B. Perkins, R.A. Olson, and R.F. Taschek, Phys. Rev. 104, 731 (1956).
- (28) M.R. Bhat, BNL 50296 (ENDF-148) June 1971.
- (29) A.M. Lane and J.E. Lynn, Proc. Phys. Soc. A70, 557 (1957).
- (30) H. Alter, private communication, 1973.
- (31) A.D. Carlson, Neutron Standards and Flux Normalization, ANL, Oct. 21-23 (1970) p. 285.
- (32) W.P. Poenitz, *ibid* p. 320.
- (33) J.B. Czirr and M.L. Stelts, Nucl. Sci. and Eng. 52, 299 (1973). See also UCRL 74447 (Rev. 1) (June 1973).
- (34) C. Lerigoleur et al. Contributions to Karlsruhe Meeting and private communication (1973). See also Saclay Report CEA-N1662.
- (35) M.P. Fricke, W.M. Lopez, S.J. Friesenhahn, A.D. Carlson, and D.G. Costello, Proc. Nuclear Data for Reactors Conference, Helsinki, paper CN26/43 (1970).
- (36) D. Kompe, Nucl. Phys. A 133, 513 (1969).
- (37) W.P. Poenitz, D. Kompe, and H.O. Menlove, J. Nucl. Eng. 22, 505 (1968).
- (38) T.S. Belanova, A.A. Van'kov, F.F. Mikhailus, and Ya. Yostavisski, At. Eng. 19, 3 (1965). Translated in J. Nucl. Eng. 20, 411 (1966).
- (39) I. Berqvist, Ark. Fys. 23, 425 (1963).
- (40) L.M. Spitz, E. Barnard, and F.D. Brooks, Nucl. Phys. A121, 655 (1968).
- (41) M.C. Moxon and E.R. Rae, Nucl. Inst. Methods, 24, 445 (1963).
- (42) E.G. Bilpuch, L.W. Weston, and H.W. Newson, Ann. Phys. 10, 455 (1960).
- (43) J.F. Barry, J. Nucl. Energy 18, 491 (1964).
- (44) M. Lindner, private communication (Feb. 1973).
- (45) J.J. Devaney, Nucl. Sci. and Eng. 51, 272 (1973).
- (46) F.J. Vaughn and H.A. Grench, Proc. Neutron Cross Sections and Technology Conference, p. 340, Knoxville (March 1971).

- (47) B. Bogart, Proc. of Neutrons Cross Sections and Technology Conference, p. 486, Washington (March 1966).
- (48) H. Pauw and A.H.W. Aten, Jr., J. Nuclear Energy 25, 457 (1971).
- (49) A. Fabry, Report BLG463, May 1972. Volume appears in contribution by W.L. Zip to the Conf. of Nuclear Data in Science and Technology, Volume II, p. 271, Paris (1972).
- (50) T.B. Ryves, J.C. Robertson, E.J. Axton, I. Goodier, and A. William, J. Nucl. Energy 20, 249 (1966).
- (51) J.C. Robertson, T.B. Ryves, E.J. Axton, I. Goodier, and A. Williams, J. Nucl. Energy 23, 205 (1969).
- (52) W.P. Poenitz, private communication (1974).
- (53) K. Rimawi and R.E. Chrien, private communication (1974).
- (54) E. Fort EANDC(E), 157U, Vol. II, p. 29 (1973).
- (55) J.A.M. DeVilliers, C.A. Engelbrecht, W.G. Vonach, and A.B. Smith, Zeitschrift f. Physik 183, 323 (1965).
- (56) E. Barnard, J.A.M. de Villiers, C.A. Engelbrecht, and D. Reitmann, Nucl. Phys. A107, 612 (1968).
- (57) A. Langsdorf, Jr., R.O. Lane, and J.E. Monahan, ANL 5567 Rev. (1961).
- (58) J.A. Nelson, V.R. Dove, and R.M. Wilenzich, Phys. Rev/C 3, 307 (1971).
- (59) C.L. Dunford, AI-AEC-12931 (1973).
- (60) Nuclear Level Schemes A=45 through A=257 from Nuclear Data Sheets, edited by Nuclear Data Group, Academic Press Inc. (New York, 1973).
- (61) E. Barnard, J.A.M. DeVilliers, C.A. Engelbrecht, and D. Reitmann, Nucl. Phys. A167, 511 (1971).
- (62) A.H. Wapstra and N.B. Gove, Nuclear Data Tables 9, 265 (1971).
- (63) H.A. Tewes, A.A. Caretto, A.E. Miller, and D.R. Nethaway, private communication (1960).
- (64) R.J. Prestwood and B.P. Bayhurst, Phys. Rev. 121, 1438 (1961).
- (65) W. Dilge, H. Vonach, G. Winkler, and P. Hille, Nucl. Phys. A118, 9 (1968).
- (66) S.M. Qaim, Nucl. Phys. A185, 614 (1972).

- (67) A.K. Hankla, R.W. Fink, and J.H. Hamilton, Nucl. Phys. A180, 157 (1972).
- (68) D.R. Nethaway, Nucl. Phys. A190, 635 (1972).
- (69) D.S. Mather, P.F. Bampton, R.E. Coles, G. James, P.J. Nind, Aldermaston Report No. AWRE10-72/72 (Nov. 1972).
- (70) H. Liskien, EANDC(E), 157U(1) (March 1973).
- (71) B.P. Bayhurst and R.J. Prestwood, J. Inorg. Nuclear Chem. 23, 173 (1961).
- (72) R.F. Coleman, B.E. Hawker, L.P. O'Connor, and J.L. Perkins, Proc. Phys. Soc. 73, 215 (1959).
- (73) G.M. Marcazzan, F. Tonolini, and L. Zetta, Nucl. Phys. 46, 51 (1963).
- (74) H. Kitazawa, Nucl. Phys. A149, 513 (1970).
- (75) B. Holmqvist and T. Wiedling, Nucl. Phys. A188, 24 (1972) and Report AE-403 (1971) plus private communication.
- (76) S.G. Buccino, C.E. Hollandsworth, and P.R. Bevington, Zeitschrift f. Physik 196, 103 (1966).
- (77) F.T. Kuchnir, A.J. Elwyn, J.E. Monahan, A. Langsdorf, Jr., and F.P. Mooring, Phys. Rev. 176, 1405 (1968).
- (78) M. Walt and J.R. Beyster, Phys. Rev. 98, 677 (1955).
- (79) M. Walt and H.H. Barshall, Phys. Rev. 93, 1062 (1954).
- (80) E.H. Auerbach, ABACUS-2 (Rev. BNL 6562 (1962)).
- (81) R.R. Kinsey, DUMMY-5, private communication (1972).
- (82) K.R. Alvar, Nucl. Phys. A 195, 289 (1972).
- (83) M. Bormann, W. Schmidt, V. Schröder, W. Scobel, and U. Seebeck, Nucl. Phys. A186, 65 (1972).
- (84) V.B. Anufrienko, Sov. J. Nucl. Phys. 2, 589 (1966).
- (85) J.J. Griffin, Phys. Rev. Letters 17, 478 (1966).
- (86) M. Blann, Phys. Rev. Letters 27, 337 (1971).
- (87) C.K. Cline and M. Blann, Nucl. Phys. A172, 225 (1971).
- (88) W. Dilge, W. Mannhart, E. Steichele, and P. Arnold, Z. Physik 264, 427 (1973).
